Modification of the Phase Stability of Polymer Blends by Diblock Copolymer Additives

3 **AUTHORS**, INCLUDING:

Karl F. Freed
University of Chicago
657 PUBLICATIONS **16,394** CITATIONS

SEE PROFILE

J. F. Douglas
National Institute of Standards and Technology
428 PUBLICATIONS **14,795** CITATIONS

SEE PROFILE

Modification of the Phase Stability of Polymer Blends by Diblock Copolymer Additives

Jacek Dudowicz,[†] Karl F. Freed,*,[†] and Jack F. Douglas[‡]

The James Franck Institute and the Department of Chemistry, University of Chicago, Chicago, Illinois 60637, and Polymers Division, National Institute of Standards and Technology, Gaithersburg, Maryland 20899

ABSTRACT: The addition of a third component to a binary mixture usually alters the critical temperature and critical composition for phase separation. In practice, these shifts can be large, leading to both increasing and decreasing of the phase stability of the mixture. Lattice cluster theory calculations show that the addition of a small amount of A-*b*-B diblock copolymer to an A/B polymer blend shifts the phase boundary as "impurities" do in other fluid mixtures. The novel feature associated with the dilution of the blend by a diblock copolymer additive is that both stabilization and destabilization can be achieved for certain conditions merely by "tuning" the asymmetry of the block lengths in the diblock copolymer. More substantial shifts are found in the phase diagram of a blend [polystyrene/poly(vinyl methyl ether)] exhibiting a lower critical solution temperature. We also examine the relation between the shifts in the critical temperature and in the critical composition of the blend in order to compare with a phenomenological relation which is observed to apply for small molecule diluted mixtures. The shift of the critical temperature is found to be approximately linearly related to the critical composition shift when the block copolymer is nearly symmetric, but no simple relation seems to exist for asymmetric diblock copolymers.

I. Introduction

It is usually difficult to produce thermodynamically stable polymer blends of high molecular weight polymers, since the entropy of mixing for these systems is rendered very small because of chain connectivity.[1] As a consequence, commercial blends are often prepared in a nonequilibrium state by mechanical mixing. The success of this approach relies on the sluggish dynamics of phase separation in high molecular weight polymers. Apart from the problem of the long term stability of such blends, the mechanical and transport properties of these mixtures often deviate considerably from the optimal combinations derived from the properties of the individual mixture components.

It has been long appreciated[2] that these mechanically mixed systems may be "compatibilized" by adding copolymers having the same chemical composition as the homopolymer blend. The copolymers further improve the adhesion between the phases and inhibit the coalescence between the phases[3] through the reduction of the interfacial tension. Recent works have emphasized this type of compatibilization effect by block copolymers[4,5] and other "surfactants".[6] The enhanced properties and commercial success of blends modified by block copolymer additives motivate the continued investigation of this strategy for forming more stable blends with improved and controlled properties.

The addition of a diblock copolymer to a polymer blend has thermodynamic implications beyond the resultant "frustration" of the phase separation process. When polymer blends are miscible or are only marginally incompatible, the dilution of the blend by a diblock copolymer can strongly influence the phase stability of the blend. This kind of dilution effect is common to any type of additive to a fluid mixture. Dilution of a fluid mixture even by small amounts of a third component (often called an "impurity") can produce dramatically large shifts of phase boundaries toward either greater

or less phase stability. The most careful studies exist for methanol–cyclohexane mixtures with water or acetone as the impurity.[7–9] There seems to be very little quantitative investigation of this phenomenon for polymer blends and polymer solutions even with the use of small molecule impurities, although there are numerous references to observed large qualitative shifts of the phase boundary for diluted blends and solutions.[10]

A phenomenological mixing rule of Timmermans[8,11,12] indicates that additives, which are soluble in both components of the fluid mixture, tend to stabilize the mixture [i.e., tend to decrease the critical temperature of an upper critical solution temperature (UCST) type phase separation], while additives which are more soluble in one component of the fluid mixture tend to destabilize the system. Many examples of this "rule of thumb" have been observed,[12] but remarkably, there is little theoretical investigation of this general phenomenon. More recently, another striking regularity has been found for the influence of additives on the phase diagram of fluid mixtures. Experiments with several small molecule fluid mixtures[7–9] show that the shift of the critical temperature, $\Delta T_c \equiv T_c(\Phi_3) - T_c(\Phi_3=0)$, where Φ_3 is the concentration (volume fraction in the present paper) of the additive, is proportional to the shift in the critical composition, $\Delta\Phi_1^{(c)} \equiv \Phi_1^{(c)}(\Phi_3) - \Phi_1^{(c)}(\Phi_3 = 0)$. In particular, the simple relation,

$$\Delta T_c/T_c(\Phi_3=0) \approx \Delta\Phi_1^{(c)}/\Phi_1^{(c)}(\Phi_3=0) \qquad (1.1)$$

is found to apply as a good approximation. It certainly would be convenient from an experimental standpoint if eq 1.1 were valid and the shift in the critical composition with dilution could be inferred simply from the corresponding shift of the critical temperature.

The utilization of additives to alter the thermodynamics of mixing offers an alternative strategy for fabricating (thermodynamically) stable blends. This possibility depends subtly on the interaction between the additive and the homopolymers and on the shape of the additive molecule, so that the choice of additive

to control miscibility has been a matter of art. The present paper employs the lattice cluster theory[13] (LCT) for polymer blends to understand the applicability to these systems of various empirical mixing rules, such as the Timmermans rule mentioned above. The study is designed to facilate a more rational choice of optimal additives. The Timmermans rule is very interesting in the context of blend dilution by diblock copolymers since it suggests that both stabilization and destabilization of the blend should occur depending on the molecular weight asymmetry of the diblock copolymer. Such a phenomenon is expected because the symmetric diblock should be soluble in both symmetric homopolymer phases by construction (provided the block copolymer concentration is not high enough for micelle formation), while the asymmetric diblock should evidently be more soluble in the homopolymer blend component corresponding to the longer block of copolymer. This expected behavior is found from the lattice cluster theory calculations for specific examples of block copolymers [polystyrene–poly(methyl methacrylate) diblock copolymers (PS-*b*-PMMA) and the isotopic diblock PSD-*b*-PSH copolymers], but the trend is not *universal*. An examination of the PS/PVME [poly(vinyl methyl ether)] blend shows a very strong blend destabilization upon the addition of the PS-*b*-PVME diblock copolymer even for a symmetric diblock. While the PS-*b*-PVME diblock has not yet been synthesized, this result should apply to other lower critical solution temperature (LCST) blends.

Section II outlines the theoretical background by defining the stability conditions for constant pressure ternary systems and by briefly describing the generalization of the lattice cluster theory to polymer blends diluted by diblock copolymers. The technical lattice cluster theory details of calculating free energy for such a three component mixture are provided in the Appendix. Section III analyzes the computed spinodal curves for the three representative examples and discusses the validity of the empirical relation, eq 1.1, for these systems. We illustrate the phase behavior through computations of the spinodals because of the enormous technical complexity in computing coexistence surfaces for ternary systems and because experiments for ternary systems rarely consider the binodals.

II. Lattice Cluster Theory for a Polymer Blend Diluted by Diblock Copolymer

A. Model of Block Copolymer Diluted Blend. The ternary mixture A/B/A-*b*-B consists of homopolymers A and B and an A-*b*-B diblock copolymer whose blocks contain the same monomers as in the homopolymer chains. The polymers A, B, and A-*b*-B are also designated by the indices 1, 2, and 3, respectively, for convenient use in summations, etc. The junction between two blocks is assumed to be provided by a single bond for simplicity. The present model depicts this three-component system by a set of $n = n_1 + n_2 + n_3$ polymer chains placed on a regular array of N_1 total lattice sites and coordination number z in such a way that each monomer of a given species α (α = A and B) has a specified molecular structure and occupies s_α lattice sites. The structures for A and B monomers are chosen to most closely corresponding to the united atom models, and the numbers s_A and s_B reflect the relative monomer sizes. Examples of monomer structures used in our calculations are presented in Figure 1, and consecutive monomers are joined together by flexible backbone bonds.
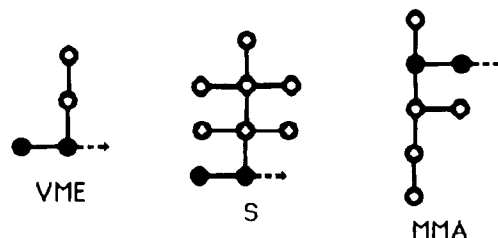

Figure 1. Monomer structure models for vinyl methyl ether (VME), styrene (S), and methyl methacrylate (MMA). Circles denote monomer portions that occupy single lattice sites, and lines depict bonds which are fully flexible in three-dimensional space. Solid circles represent monomer portions lying on the chain backbone, and the arrows indicate the directions of linkages between consecutive monomers in the polymer chains.

Each homopolymer chain of component i contains N_i monomers and extends over $M_i = N_i s_i$ lattice sites, where $s_1 = s_A$ and $s_2 = s_B$, while the chain occupancy index for the A-*b*-B diblock copolymer is the sum of the contributions from the two blocks, i.e., $M_3 = N_b^{(A)} s_A + N_b^{(B)} s_B$ where $N_b^{(A)}$ and $N_b^{(B)}$ are the polymerization indices of blocks A and B, respectively. The compressibility of this ternary polymer blend arises from the presence of excess free volume which is introduced into the model by allowing n_v lattice sites to be empty. The vacant volume fraction $\phi_v = n_v/(n_1 M_1 + n_2 M_2 + n_3 M_3 + n_v) = n_v/N_1$ emerges as a measure of the excess free volume and is determined from the equation of state for given pressure, temperature, and blend composition. The composition of the compressible ternary blend is expressed either in terms of the actual volume fractions $\phi_i = n_i M_i/N_1$ (normalized as $\phi_1 + \phi_2 + \phi_3 + \phi_v = 1$) or the nominal volume fractions $\Phi_i = \phi_i/(1 - \phi_v)$ satisfying the condition $\Phi_1 + \Phi_2 + \Phi_3 = 1$. The model employs a three-dimensional $z = 2d = 6$ cubic lattice whose unit volume v_{cell} (associated with one lattice site) is assumed to be constant.

As in small molecule fluids, the interactions in polymer blends involve short range repulsions and longer range attractions. While the former are described in the lattice model by the excluded volume constraints that no two submonomer segments occupy the same lattice site, the latter are introduced by assigning the attractive microscopic van der Waals energy $\epsilon_{\alpha\beta}^{ij}$ to nearest neighbor portions i and j of monomers α and β, respectively. All s_α portions of a given monomer α are taken as energetically equivalent groups which interact with a submonomer unit of a monomer β by the same microscopic energy $\epsilon_{\alpha\beta}$. This simplification leads in our case to the presence of three independent energies ϵ_{AA}, ϵ_{BB}, and ϵ_{AB}, which represent the minimum number of energetic parameters for treating a compressible A/B/A-*b*-B blend. Generally, different chemical groups interact with varying energies. However, such a multi-energy description of ternary systems becomes rather complex and requires numerous adjustable parameters. Thus, we idealize the more complex situation by using just three averaged interaction energies.

B. Free Energy of a Block Copolymer Diluted Blend. The lattice cluster theory[13] (LCT) provides the Helmholtz free energy F for a ternary A/B/A-*b*-B polymer blend as

$$\frac{F}{N_l k_B T} = \phi_v \ln \phi_v + \sum_{i=1}^{i=3} \frac{\phi_i}{M_i} \ln \frac{2\phi_i}{M_i} - (\ln z - 1)\sum_{i=1}^{i=3}\left(1 - \right.$$

$$\left.\frac{1}{M_i}\right)\phi_i + \sum_{k=1}^{k^*}\sum_{l=0}^{k}[f_{lk}^{(1,2)}\phi_1{}^l\phi_2{}^{k-l} + f_{lk}^{(1,3)}\phi_1{}^l\phi_3{}^{k-l} + $$

$$f_{lk}^{(2,3)}\phi_2{}^l\phi_3{}^{k-l}] + \sum_{k=1}^{k^*}\sum_{l=1}^{k^*-k-1}\sum_{m=1}^{k^*-k-l} f_{mlk}^{(1,2,3)}\phi_1{}^m\phi_2{}^l\phi_3{}^k \quad (2.1)$$

where the last two terms on the right-hand side of eq 2.1 represent the noncombinatorial part of F as a polynomial in the actual volume fractions and where the summation indices m, l, and k range over A, B, and A-b-B which are designated in eq 2.1 as 1, 2, and 3, respectively. The double summation term in eq 2.1 is the pairwise additive portion of the noncombinatorial free energy F_{nc} from the three binary systems A/B, A/A-b-B, and B/A-b-B, while the triple summation term in eq 2.1 corresponds to the nonadditive portion of F_{nc} that arises from correlations between all three polymer species. Equation 2.1 illustrates the following useful feature of the cluster expansion: Our previous developments of the lattice cluster theory for the free energy of binary homopolymer blends[13,14] and binary diblock copolymer–homopolymer systems[15] can be utilized to provide the pairwise additive portion of F_{nc} for the ternary A/B/A-b-B systems. The only necessary extension of the LCT to ternary systems involves the calculation of the coefficients $f_{mlk}^{(1,2,3)}$ in the nonpairwise additive contribution. The latter are likewise obtained[13,14] as double expansions in the inverse lattice coordination number $1/z$ and in the three dimensionless microscopic van der Waals attractive energies $\epsilon_{\alpha\beta}/k_B T$. The coefficients in these double expansions depend on the monomer structures of all blend components, the diblock composition variable $f = N_b^{(A)}/(N_b^{(A)} + N_b^{(B)})$ [or rather $m = M_3^{(A)}/(M_3^{(A)} + M_3^{(B)})$], and the site occupancy indices M_1, M_2, and $M_3 \equiv N_b^{(A)}s_A + N_b^{(B)}s_B$. The present calculations of F are performed only through orders $1/z^2$ and $(\epsilon_{\alpha\beta}/k_B T)$, and this fixes[13] the upper limit of k in the double and triple summations in eq 2.1 as $k^* = 5$.

While the Helmholtz free energy F is most appropriate for treating the thermodynamics of systems at constant volume V, blends at constant pressure P are most conveniently described by the Gibbs free energy G,

$$G = F + PV = F + PN_l v_{cell} \quad (2.2)$$

where the pressure P is computed from the standard relation as

$$P \equiv -\left.\frac{\partial F}{\partial V}\right|_{T,n_1,n_2,n_3} = -\frac{1}{v_{cell}}\left.\frac{\partial F}{\partial n_v}\right|_{T,n_1,n_2,n_3} \quad (2.3)$$

Since the unit volume v_{cell} associated with one lattice site is assumed to be constant, the total volume $V = N_l v_{cell}$ of the lattice containing n_1, n_2, and n_3 chains of three different polymer species can be changed only by varying the number of voids. The equation of state is derived from eqs 2.3 and 2.1 and enables a determination of the free volume fraction $\phi_v = \phi_v(P,T,\Phi_1,\Phi_2)$. Usually, the cell volume v_{cell} is estimated from the specific monomer volumes $v'_\alpha = v_\alpha/s_\alpha$ as

$$v_{cell} = (v'_A v'_B)^{1/2} \quad (2.4)$$

The choice of (2.4), however, does not influence the

magnitude of the calculated void volume fraction ϕ_v and free energy (2.2). Both of these quantities display almost no sensitivity to v_{cell} over very wide ranges of pressures and temperatures.

C. Stability of Block Copolymer Diluted Blends. Generally, a ternary system at constant pressure P and temperature T is stable (or metastable)[16] if

$$\left.\frac{\partial^2 g}{\partial X_1{}^2}\right|_{P,T,X_2}\left.\frac{\partial^2 g}{\partial X_2{}^2}\right|_{P,T,X_1} - \left[\left.\frac{\partial^2 g}{\partial X_1 \partial X_2}\right|_{P,T}\right]^2 > 0 \quad (2.5)$$

where g designates the specific Gibbs free energy and $\{X_i\}$ denote the composition variables normalized such that $X_1 + X_2 + X_3 = 1$. Only two of these three X_i are independent, and eq 2.5 is written on the basis of the choice of X_1 and X_2 as the independent composition variables. Standard thermodynamic analysis shows that the normalization of g and the choice of X_i must be conjugate.[17] If, for instance, X_i is a mole fraction, g must be defined per mole, if X_i is a weight fraction, g should be related to 1 g, etc. Since the polymer blend compositions are specified here by the nominal volume fractions,

$$\Phi_i = \frac{n_i M_i}{n_1 M_1 + n_2 M_2 + n_3 M_3} = \frac{n_i M_i}{N_{occ}} \quad (2.6)$$

the free energy g of eq 2.5 must be expressed per occupied lattice site (or equivalently per unit of occupied volume $V_{occ} = N_{occ}v_{cell}$); i.e., we should use $g = G/N_{occ}$ (or $g = G/V_{occ}$). A constant number N_{occ} of occupied sites corresponds in a continuum system to a constant quantity of polymers. Equating the left-hand side of the inequality (2.5) to zero yields the stability limit (called the "spinodal") for the constant pressure ternary polymer blend,

$$\left.\frac{\partial^2 g}{\partial \Phi_1{}^2}\right|_{P,T,\Phi_2}\left.\frac{\partial^2 g}{\partial \Phi_2{}^2}\right|_{P,T,\Phi_1} - \left[\left.\frac{\partial^2 g}{\partial \Phi_1 \partial \Phi_2}\right|_{P,T}\right]^2 = 0 \text{ (spinodal)} \quad (2.7)$$

Equation 2.7 produces a set of temperatures $\{T_s\}$ for a given blend composition $\{\Phi_1, \Phi_2\}$. Hence, the full spinodal for a ternary system is represented by a surface $T_s = T_s(\Phi_1,\Phi_2)$, while a curve $T_s = T_s(\Phi_1)$ refers to the simpler case of constant Φ_3 (or Φ_2).

For computational convenience, the condition of eq 2.7 is converted to the form

$$\left.\frac{\partial(\mu_1 - \mu_3)}{\partial \Phi_1}\right|_{P,T,\Phi_2}\left.\frac{\partial(\mu_2 - \mu_3)}{\partial \Phi_2}\right|_{P,T,\Phi_1} -$$

$$\left.\frac{\partial(\mu_1 - \mu_3)}{\partial \Phi_2}\right|_{P,T,\Phi_1}\left.\frac{\partial(\mu_2 - \mu_3)}{\partial \Phi_1}\right|_{P,T,\Phi_2} = 0 \quad (2.8)$$

where the chemical potentials μ_i are defined on a per lattice site basis as

$$\mu_i = \frac{1}{M_i}\left.\frac{\partial F}{\partial n_i}\right|_{V,T,\{n_{j\neq i}\}} = \left.\frac{\partial[F/N_l]}{\partial \phi_i}\right|_{N_l,T,\{\phi_{j\neq i}\}} \quad i,j = 1-3 \quad (2.9a)$$

$$= \frac{1}{M_i}\left.\frac{\partial G}{\partial n_i}\right|_{P,T,\{n_{j\neq i}\}} \quad (2.9b)$$

and the free energy F is provided by the LCT expansion (2.1). The appearance of the exchange chemical poten-

tials

$$\mu_1 - \mu_3 = \frac{\partial g}{\partial \Phi_1}\bigg|_{P,T,\Phi_2} \quad (2.9c)$$

and

$$\mu_2 - \mu_3 = \frac{\partial g}{\partial \Phi_2}\bigg|_{P,T,\Phi_1} \quad (2.9d)$$

in eq 2.8 can be understood by introducing the constraint of constant N_{occ} into the well-known indentity

$$dG = \sum_{i=1}^{i=3} \mu_i M_i dn_i \qquad P, T = \text{const} \quad (2.9e)$$

Having written eq 2.7 in terms of chemical potential derivatives, further simplifications of eq 2.8 are possible since variations of the intensive quantities μ_i are not independent but are connected to each other by the Gibbs–Duhem relations,

$$\sum_{i=1}^{i=3} \Phi_i \frac{\partial \mu_i}{\partial \Phi_j}\bigg|_{P,T,\Phi_{k\neq j}} = 0 \qquad j = 1 \text{ and } 2 \quad (2.10)$$

The final form of the spinodal condition

$$\frac{\partial \mu_1}{\partial \Phi_1}\bigg|_{P,T,\Phi_2}\frac{\partial \mu_2}{\partial \Phi_2}\bigg|_{P,T,\Phi_1} - \frac{\partial \mu_1}{\partial \Phi_2}\bigg|_{P,T,\Phi_1}\frac{\partial \mu_2}{\partial \Phi_1}\bigg|_{P,T,\Phi_2} = 0 \quad (2.11)$$

is much more suitable for numerical analysis than are eqs 2.8 and 2.7. Our numerical calculations of the stability limits are specialized to ternary polymer blends with a constant volume fraction Φ_3 for the diblock component. The critical point ($T = T_c$, $\Phi_1 = \Phi_1^{(c)}$) for such blends corresponds to the maximum (or minimum) on the spinodal curve $T_s = T_s(\Phi_1)$, and the condition for its existence simply follows from eq 2.11 as

$$\frac{\partial^2 \mu_1}{\partial \Phi_1^2}\bigg|_{P,T,\Phi_2}\frac{\partial \mu_2}{\partial \Phi_2}\bigg|_{P,T,\Phi_1} + \frac{\partial^2 \mu_2}{\partial \Phi_1 \Phi_2}\bigg|_{P,T}\frac{\partial \mu_1}{\partial \Phi_1}\bigg|_{P,T,\Phi_2} -$$
$$\frac{\partial^2 \mu_1}{\partial \Phi_1 \Phi_2}\bigg|_{P,T}\frac{\partial \mu_2}{\partial \Phi_1}\bigg|_{P,T,\Phi_2} - \frac{\partial^2 \mu_2}{\partial \Phi_1^2}\bigg|_{P,T,\Phi_2}\frac{\partial \mu_1}{\partial \Phi_2}\bigg|_{P,T,\Phi_1} = 0 \quad (2.12)$$

The constant pressure derivatives $\partial \mu_i/\partial \Phi_j$, $\partial^2 \mu_i/\partial \Phi_j^2$, or $\partial^2 \mu_i/\partial \Phi_i \Phi_j$ in eqs 2.11 and 2.12 are evaluated from eq 2.9a and from the equation of state (2.3) along the lines derived[18] previously by us for binary blends.

III. LCT Computations of Stability Limits for PS/PVME/PS-*b*-PVME, PS/PMMA/PS-*b*-PMMA, and PSD/PSH/PSD-*b*-PSH Ternary Blends

The LCT computations of the spinodal from eq 2.11 are performed for ternary polymer blends at the constant pressure $P = 1.013 \times 10^5$ Pa and a constant volume fraction Φ_3 of the diblock copolymer. Focusing on the $T_s = T_s(\Phi_1, \Phi_3 = \text{const})$ spinodal curves instead of on the whole spinodal surface $T_s = T_s(\Phi_1, \Phi_2)$ greatly facilitates graphical visualization and hence the analysis of the miscibility exhibited by a binary A/B blend that is diluted by an A-*b*-B diblock copolymer. The computations summarized here are based on the generalized lattice model in which molecular structures for both types of monomers extend over a few lattice sites, as
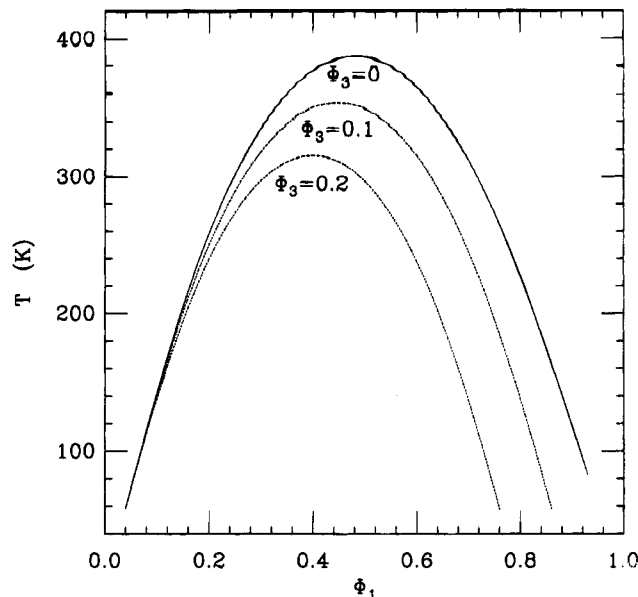

Figure 2. LCT spinodal curves for fully symmetric PS/PMMA/PS-*b*-PMMA diluted blends with $N_1 = N_2 = N_b^{(A)} = N_b^{(B)} = 50$ at constant pressure $P = 1.013 \times 10^5$ Pa and constant volume fraction Φ_3 of the PS-*b*-PMMA diblock copolymer, as indicated in the figure. The microscopic attractive van der Waals energies are taken from our previous fit[21] as $\epsilon_{S-S} = 0.5k_BT_o$, $\epsilon_{MMA-MMA} = 0.4753k_BT_o$, and $\epsilon_{S-MMA} = 0.486445k_BT_o$ ($T_o = 415.15$ K). All subsequent figures for PS/PMMA blends diluted by the PS-*b*-PMMA diblock copolymer are obtained for the same $\{\epsilon_{\alpha\beta}\}$, the pressure P of 1.013×10^5 Pa, the same polymerization indices N_1 and N_2 of the two hompolymers, and the same total polymerization index $N_3 \equiv N_b^{(A)} + N_b^{(B)}$ of the PS-*b*-PMMA diblock. Component 1 is *PS*.

depicted in Figure 1. The choice of the three particular blends PS/PVME/PS-*b*-PVME, PS/PMMA/PS-*b*-PMMA, and PSD/PSH/PSD-*b*-PSH is dictated by the availability of the energy parameters $\{\epsilon_{\alpha\beta}\}$ which have been fit using the lattice cluster theory to a wide variety of neutron-scattering and thermodynamic properties for the PS/PVME, PSD/PSH, and PS-*b*-PMMA systems.[19-21] (The large number of significant figures quoted for the $\epsilon_{\alpha\beta}$ emerge from the fitting procedure.[19-21]) We assume that all these microscopic $\{\epsilon_{\alpha\beta}\}$ are transferable from binary homopolymer blends A/B to the corresponding diblock copolymers A-*b*-B (and vice versa) and that they remain unchanged when used to represent interactions in ternary A/B/A-*b*-B blends. These three blends are also selected because their phase diagrams exhibit a large range of behaviors, as described below.

The first example is provided by the PS/PMMA/PS-*b*-PMMA system whose stability limits are illustrated in Figure 2 for completely symmetric polymerization indices $N_{PS} = N_{PMMA} = N_{PS}^{(A)} = N_{PMMA}^{(B)} = 50$ (and, therefore, a symmetric diblock composition variable $f = N_{PS}/(N_{PS}^{(A)} + N_{PMMA}^{(B)}) = 1/2$). The notation employed in Figure 2 and all subsequent figures is that Φ_1 is the volume fraction for component A of the A/B/A-*b*-B ternary system. Figure 2 demonstrates that the addition of a symmetric PS-*b*-PMMA diblock into a binary PS/PMMA blend favors blend miscibility. Significant amounts of diblock ($\Phi_3 \approx 0.1$) are necessary to decrease the critical temperature by about 10%. (On an absolute temperature scale this amounts to a rather significant shift $O(30 \text{ }^\circ\text{C})$ of the phase boundary for mixtures which phase separate at temperatures near room temperature.) A similar behavior is found for the PSD/PSH/PSD-*b*-PSH system, as shown in Figure 3. The latter system provides a useful illustration because its high degree of compatibility permits the consideration of
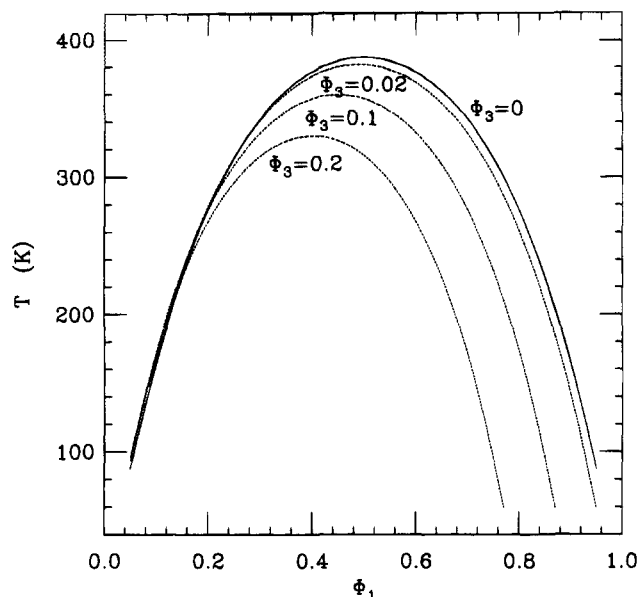
Figure 3. LCT spinodal curves for fully symmetric PSD/PSH/PSD-b-PSH diluted blends with $N_1 = N_2 = N_b^{(A)} = N_b^{(B)} = 10^4$ at constant pressure $P = 1.013 \times 10^5$ Pa and constant volume fraction Φ_3 of the PSD-b-PSH diblock copolymer, as indicated in the figure. The microscopic attractive van der Waals energies are taken from our previous fit[20] as $\epsilon_{SD-SD} = 0.5k_BT_o$, $\epsilon_{SH-SH} = 0.501k_BT_o$, and $\epsilon_{SD-SH} = 0.5004925k_BT_o$ ($T_o = 415.15$ K). All subsequent figures for *PSD/PSH* blends diluted by the PSD-b-PSH diblock copolymer are obtained for the same $\{\epsilon_{\alpha\beta}\}$, the pressure P of 1.013×10^5 Pa, and, if not otherwise stated, the same polymerization indices N_1 and N_2 of the two homopolymers and for the same total polymerization index N_3 $\equiv N_b^{(A)} + N_b^{(B)}$ of the PSD-b-PSH diblock. Component 1 is PSD.

examples with rather large polymerization indices. The above results are not unexpected since the phase separation in both the PS/PMMA and PSD/PSH binary blends (as in all UCST systems) is energetically driven. Thus, rather large quantities of diblock are required to balance unfavorable heterocontact interactions.

A rather different influence of a diblock copolymer on blend miscibility appears in Figure 4 which presents computed spinodal curves $T_s = T_s(\Phi_1, \Phi_3 = \text{const})$ for a PS/PVME/PS-b-PVME blend with $N_{PS} = N_{PVME} = N_{PS}^{(A)} = N_{PVME}^{(B)} = 10^3$. In contrast to the stabilizing effects of PS-b-PMMA or PSD-b-PSH diblock copolymers, quite miniscule amounts of PS-b-PVME (Φ_3 of order 10^{-4}) are sufficient to yield a substantial shift in the spinodal of the binary PS/PVME blend. The pure binary blend ($\Phi_3 = 0$) spinodal has only a lower critical solution temperature (LCST), but the ternary systems in Figure 4 all exhibit *both* lower and upper critical solution temperatures, with the topmost of the solid curves and bottommost of the dashed curves corresponding to the same Φ_3. A possible explanation for the behavior in Figure 4 emerges from the fact that the phase separation in PS/PVME blends is entropically driven, and the addition of small quantities of a diblock copolymer introduces a significant perturbation to the system entropy.

Computations are readily performed to investigate the variation of Figures 2–4 with changes in the polymerization index. Examples are provided now for the symmetric case of $N \equiv N_A = N_B = N^{(A)} = N^{(B)}$. As N increases from 500 to 5000, the diblock fraction Φ_3 of PS-b-PVME necessary to produce a critical temperature shift $\Delta T_c(\Phi_3) \approx 140$ K decreases considerably from $\Phi_3 = 5.8 \times 10^{-4}$ to 5.3×10^{-5}. The UCST phase diagrams require much more diblock additive to provide interest-
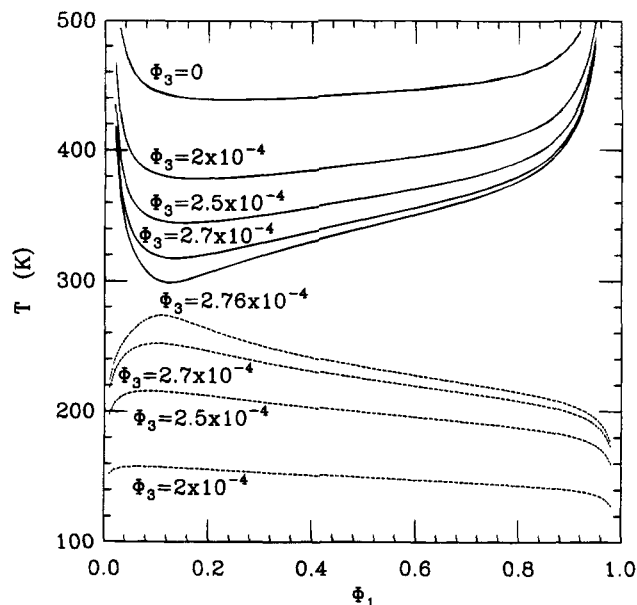

Figure 4. LCT spinodal curves for fully symmetric PS/PVME/PS-b-PVME diluted blends with $N_1 = N_2 = N_b^{(A)} = N_b^{(B)} = 10^3$ at constant pressure $P = 1.013 \times 10^5$ Pa and constant volume fraction Φ_3 of the PS-b-PVME diblock copolymer, as indicated in the figure. The microscopic attractive van der Waals energies are taken from our previous fits[19] as $\epsilon_{S-S} = 0.5k_BT_o$, $\epsilon_{VME-VME} = 0.56k_BT_o$, and $\epsilon_{S-VME} = 0.533605k_BT_o$ ($T_o = 415.15$ K). Component 1 is *PS*.

ing shifts ΔT_c. Hence, these cases are illustrated for $\Phi_3 = 0.2$. Changing N from 50 to 80 for the PS/PMMA system converts ΔT_c from 72 to 105 K, respectively. The corresponding values for the PSD/PSH system are $\Delta T_c(0.2) = 55$ K for $N = 10^4$ and $\Delta T_c(0.2) = 60$ K for $N = 2 \times 10^4$. In general, higher N produces a larger ΔT_c at fixed Φ_3 or, equivalently, a smaller Φ_3 is necessary to yield a given ΔT_c as N increases.

While the computations summarized in Figures 2–4 refer to symmetric blends diluted by symmetric diblock copolymers with the polymerization indices $N_b^{(A)}$ and $N_b^{(B)}$ equal to each other (and hence the composition variable $f = \frac{1}{2}$) and with identical polymerization indices N_1 and N_2 of the homopolymer species 1 and 2, practical questions center on whether the use of *unsymmetric* diblocks enables exerting substantial control on the phase diagram. Figures 5 and 6 answer this important question by delineating, respectively, the spinodal curves for PS/PMMA/PS-b-PMMA and PSD/PSH/PSD-b-PSH blends with different diblock compositions f, a constant volume fraction $\Phi_3 = 0.05$, and the same polymerization indices N_1, N_2, and $N_3 \equiv N_b^{(A)} + N_b^{(B)}$ as in Figures 2 and 3. Figures 5 and 6 also provide curves for a symmetric diblock ($f = \frac{1}{2}$) which produces the above discussed blend stabilization, but the remaining curves show that the asymmetric diblocks with $f = 0.1$, 0.7, and 0.9 destabilize the blend at low dilution, displaying a stronger destabilization with increasing asymmetry. Since the interaction energies $\{\epsilon_{\alpha\beta}\}$ and monomer structures of PSD and PSH are much more symmetric than those representing the PS/PMMA/PS-b-PMMA system, the spinodals in Figure 6 for $f = 0.1$ and $f = 0.9$ (or for $f = 0.3$ and $f = 0.7$) exhibit almost the same shapes and the same critical temperatures. Additional LCT calculations indicate that the stabilizing effect of a symmetric A-b-B diblock copolymer is maintained when the polymerization indices of homopolymers A and B are no longer equal to each other. This result along with the examples of Figures 5 and 6
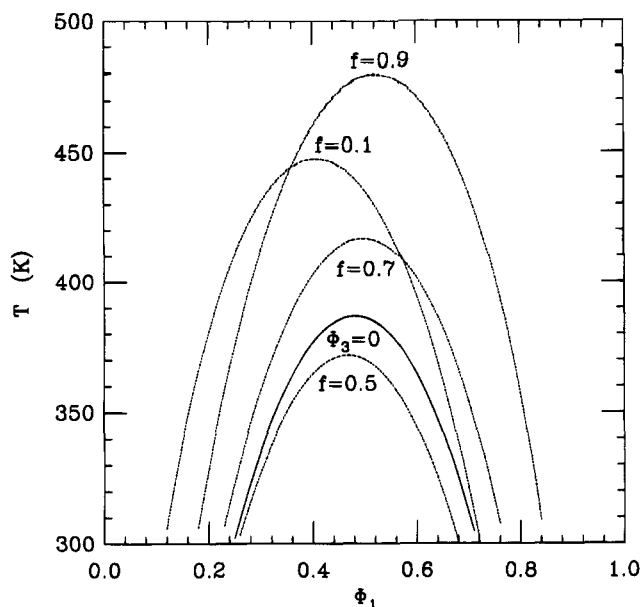
Figure 5. LCT spinodal curves for symmetric PS/PMMA/PS-*b*-PMMA ternary blends ($N_1 = N_2 = 50$ and $N_3 \equiv N_b^{(A)} + N_b^{(B)} = 100$) at constant volume fraction $\Phi_3 = 0.05$ of the PS-*b*-PMMA diblock copolymer. Different curves correspond to different values of the diblock composition variable $f \equiv N_b^{(A)}/(N_b^{(A)} + N_b^{(B)})$ for A $\equiv$ *PS*, as indicated in the figure.
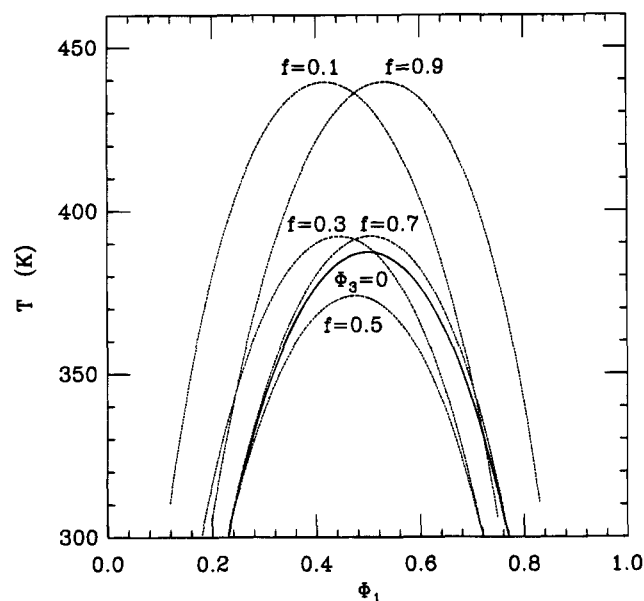

Figure 6. Same as Figure 5 but for symmetric PSD/PSH/PSD-*b*-PSH blends ($N_1 = N_2 = 10^4$, and $N_3 \equiv N_b^{(A)} + N_b^{(A)} = 2 \times 10^4$).

suggests that the relative lengths of the two blocks seem to be an important factor influencing the phase diagram of A/B/A-*b*-B polymer blends. The block lengths, therefore, cannot be neglected in the analysis of the miscibility of an A/B homopolymer blend diluted by A-*b*-B diblock copolymers.

A convenient way of analyzing the diluted blend data focuses on how the critical parameters T_c and $\Phi_1^{(c)}$ are shifted by dilution with diblock copolymers composed of the same monomers as in the homopolymer chains. Figures 7 and 8 display, respectively, the relative shifts in the critical temperature

$$\Delta T_c/T_c(\Phi_3=0) \equiv [T_c - T_c(\Phi_3=0)]/T_c(\Phi_3=0) \quad (3.1)$$
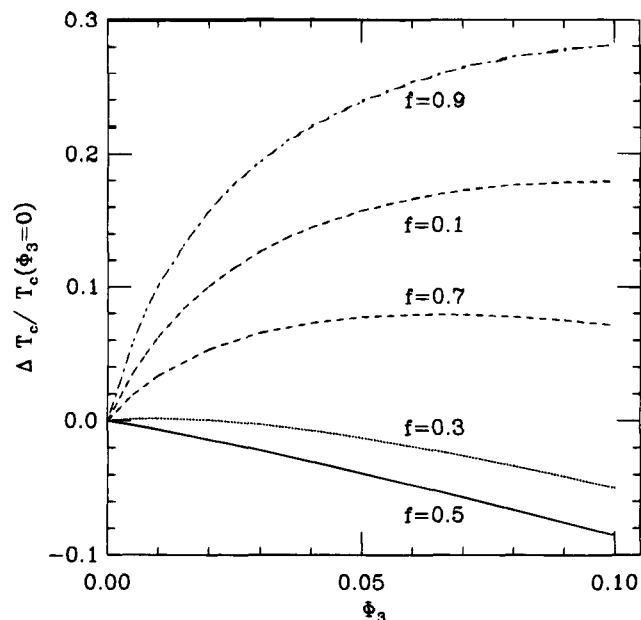
and in the critical composition

Figure 7. LCT predictions for the diblock volume fraction (Φ_3) dependence of the relative shift in the critical temperature [$T_c - T_c(\Phi_3=0)]/T_c(\Phi_3=0)$ for PS/PMMA blends diluted by PS-*b*-PMMA diblock copolymers with different compositions f and A $\equiv$ *PS*.
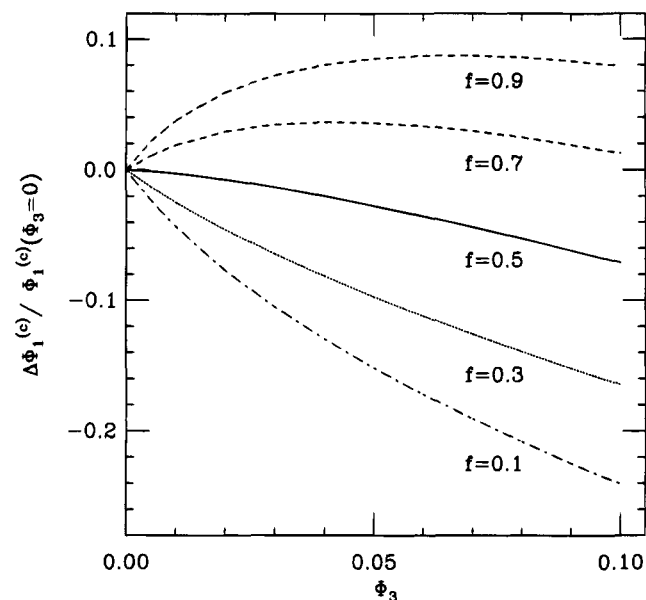

Figure 8. Same as Figure 7 but for the relative shift in the critical composition [$\Phi_1^{(c)} - \Phi_1^{(c)}(\Phi_3=0)]/\Phi_1^{(c)}(\Phi_3=0)$.

$$\Delta\Phi_1^{(c)}/\Phi_1^{(c)}(\Phi_3=0) \equiv [\Phi_1^{(c)} - \Phi_1^{(c)}(\Phi_3=0)]/\Phi_1^{(c)}(\Phi_3=0) \quad (3.2)$$

where $T_c(\Phi_3=0)$ and $\Phi_1^{(c)}(\Phi_3 = 0)$ refer to a pure ($\Phi_3=0$) binary system. Both $\Delta T_c/T_c(\Phi_3=0)$ and $\Delta\Phi_1^{(c)}/\Phi_1^{(c)}(\Phi_3 = 0)$ are presented as a function of the block copolymer volume fraction Φ_3 for a few PS/PMMA/PS-*b*-PMMA blends with different diblock compositions f, but with the same polymerization indices $N_1 = 50$, $N_2 = 50$, and $N_3 = 100$. First of all, the plots in Figures 7 and 8 indicate that both these critical quantities are very sensitive to the diblock composition f and may increase or decrease with f. Generally, $\Delta T_c/T_c(\Phi_3=0)$ and $\Delta\Phi_1^{(c)}/\Phi_1^{(c)}(\Phi_3 = 0)$ depend on Φ_3 in a nonlinear fashion, except for the symmetric case of $f = {}^1/_2$ and very short diblock chains with N_3 of order unity (see Figures 9 and 10). The linearity of $\Delta T_c/T_c(\Phi_3=0)$ vs Φ_3 degenerates,
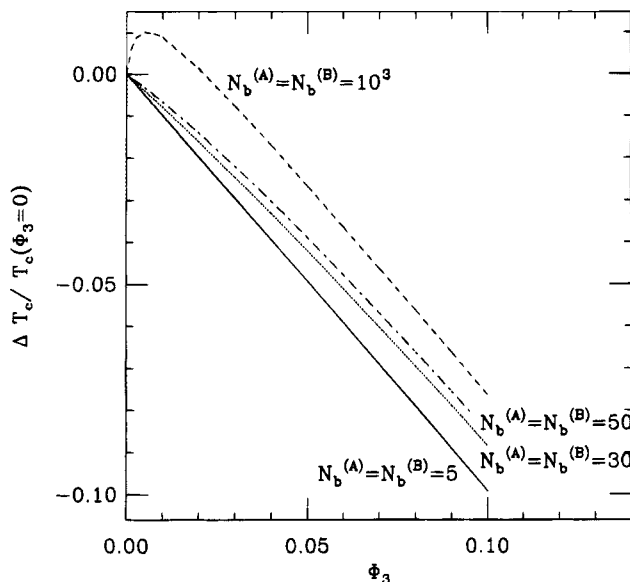
Figure 9. LCT predictions for the diblock volume fraction (Φ_3) dependence of the relative shift in the critical temperature [T_c - $T_c(\Phi_3=0)$]/$T_c(\Phi_3=0)$ for PS/PMMA blends diluted by the symmetric ($f = 1/2$) PS-b-PMMA diblock copolymer with various polymerization indices $N_b^{(A)}$ and $N_b^{(B)}$ of the two blocks, as specified in the figure.
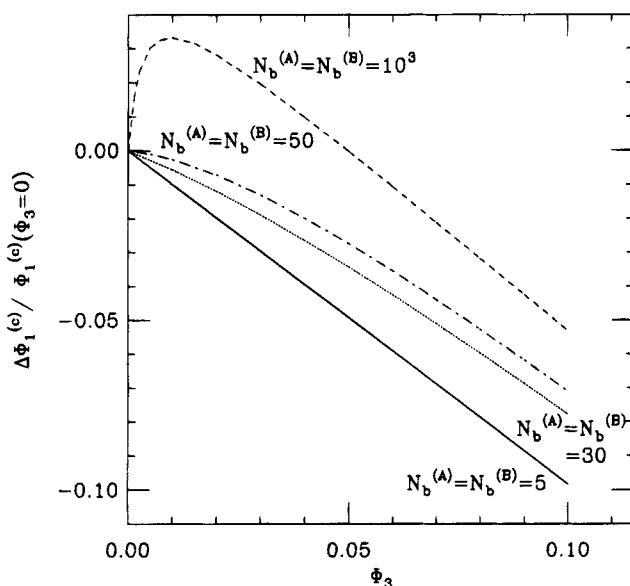

Figure 11. LCT predictions of the dependence of the relative shift in the critical temperature [T_c - $T_c(\Phi_3=0)$]/$T_c(\Phi_3=0)$ on that of the critical composition [$\Phi_1^{(c)}$ - $\Phi_1^{(c)}(\Phi_3=0)$]/$\Phi_1^{(c)}(\Phi_3=0)$ for PS/PMMA blends diluted by PS-b-PMMA diblocks with various compositions f (for A $\equiv$ PS), as indicated in the figure.

Figure 10. Same as Figure 9 but for the relative shift in the critical composition [$\Phi_1^{(c)}$ - $\Phi_1^{(c)}(\Phi_3=0)$]/$\Phi_1^{(c)}(\Phi_3=0)$.

Figure 12. LCT predictions for the dependence of the relative shift in the critical temperature [T_c - $T_c(\Phi_3=0)$]/$T_c(\Phi_3=0)$ on that of the critical composition [$\Phi_1^{(c)}$ - $\Phi_1^{(c)}(\Phi_3=0)$]/$\Phi_1^{(c)}(\Phi_3=0)$ for PS/PMMA blends diluted by symmetric ($f = 1/2$) PS-b-PMMA diblocks with various polymerization indices $N_b^{(A)}$ and $N_b^{(B)}$ of the two blocks, as specified in the figure.

however, rather slowly with an increase of block lengths. Thus, the behavior for $f = 1/2$ and $N_3 = 100$ in Figure 8 can be still considered as nearly linear. The curves in Figures 7 and 8 are combined in Figure 11 as plots of $\Delta T_c/T_c(\Phi_3=0)$ versus $\Delta\Phi_1^{(c)}/\Phi_1^{(c)}(\Phi_3 = 0)$ to enable examination of the empirical relation of eq 1.1, which describes a number of observations for small molecule liquid mixtures.[7-9] Figure 11 shows that there is only a rough linear relationship between $\Delta T_c/T_c(\Phi_3=0)$ and $\Delta\Phi_1^{(c)}/\Phi_1^{(c)}(\Phi_3 = 0)$ for symmetric ($f = 1/2$) diblocks. The validity of (1.1) is maintained, however, if the blend contains very short diblock copolymer chains ($N_b^{(A)} = N_b^{(B)} = 5$), as shown in Figure 12. The examples in Figure 11 also illustrate that the relation between the critical quantities of eqs 3.1 and 3.2 is not even roughly linear for blends diluted by asymmetric diblocks.

Similar calculations to those summarized in Figures 7–12 have been also performed for PSD/PSH/PSD-b-
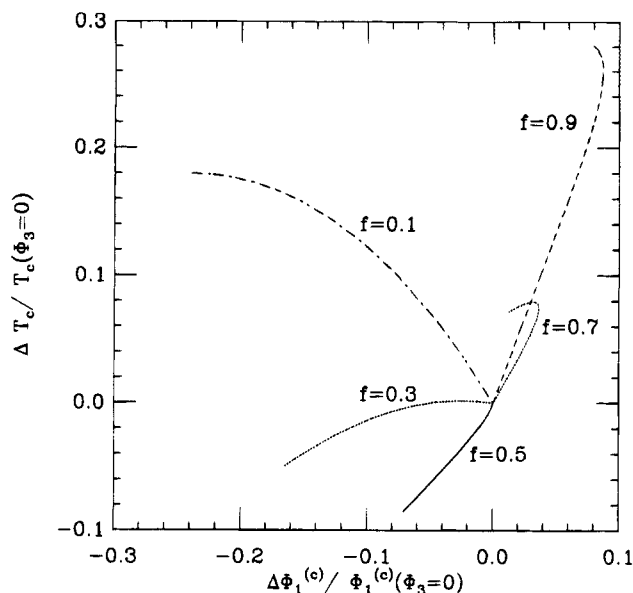
PSH blends with much larger polymerization indices $N_1 = N_2 = 10^4$ and $N_3 \equiv N_b^{(A)} + N_b^{(B)} = 2 \times 10^4$. Again, the behavior of $\Delta T_c/T_c(\Phi_3=0)$ versus $\Delta\Phi_1^{(c)}/\Phi_1^{(c)}(\Phi_3 = 0)$ appears to be linear only for $f = 1/2$. The slope departs, however, from unity and equals $\alpha = 0.708 \pm 0.003$, *independent of the diblock chain lengths*. Hence, the empirical identity (1.1) must be generalized to the form

$$\Delta T_c/T_c(\Phi_3=0) \approx \alpha[\Delta\Phi_1^{(c)}/\Phi_1^{(c)}(\Phi_3=0)] \qquad (3.3)$$

in order to apply even for symmetric PSD/PSH/PSD-b-PSH blends (with $N_1 = N_2$ and $N_b^{(A)} = N_b^{(B)}$). Introducing homopolymer polymerization index asymmetry into the LCT computations leads again to a degredation of the linear dependence of $\Delta T_c/T_c(\Phi_3=0)$ on $\Delta\Phi_1^{(c)}/\Phi_1^{(c)}$
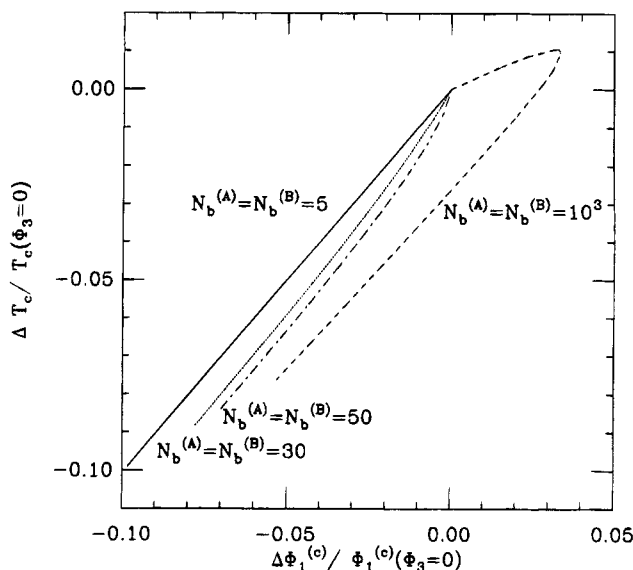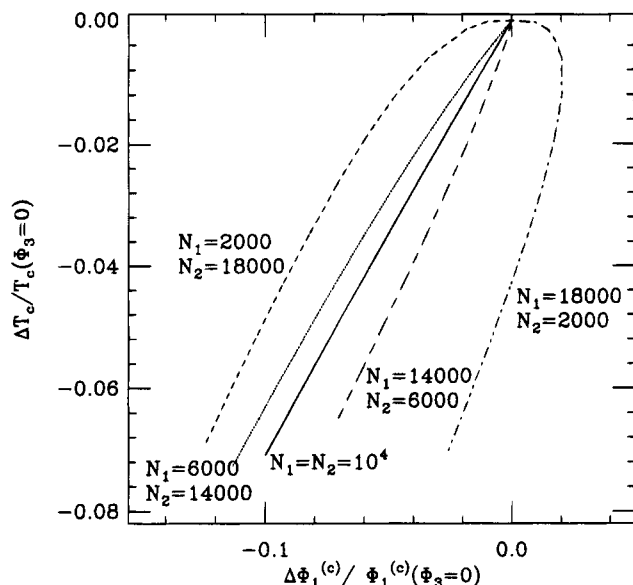
Figure 13. LCT predictions for the dependence of the relative shift in the critical temperature $[T_c - T_c(\Phi_3=0)]/T_c(\Phi_3=0)$ on that of the critical composition $[\Phi_1^{(c)} - \Phi_1^{(c)}(\Phi_3=0)]/(\Phi_1^{(c)}-(\Phi_3=0))$ for PSD/PSH blends diluted by the symmetric $(f = 1/2)$ PSD-b-PSH diblock. Different curves correspond to different polymerization indices N_1 and N_2 of both homopolymers, as indicated in the figure.
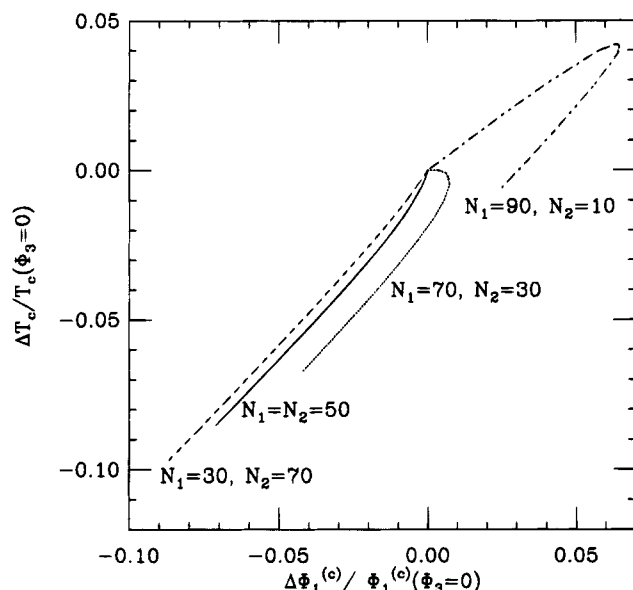

Figure 14. Same as Figure 13 but for PS/PMMA/PS-b-PMMA systems with unsymmetric polymerization indices of both homopolymers.

$\Phi_3 = 0$), as depicted in Figure 13 for PSD/PSH/PSD-b-PSH systems. Likewise, no simple correlation is found between $\Delta T_c/T_c(\Phi_3=0)$ and $\Delta\Phi_1^{(c)}/\Phi_1^{(c)}(\Phi_3 = 0)$ for asymmetric $(N_1 \neq N_2)$ PS/PMMA/PS-b-PMMA blends (see Figure 14). However, a rough linearity exists when the blend components are nearly symmetric.

All the above LCT predictions for the miscibility of A/B binary blends diluted by A-b-B diblock copolymers can easily be extended to consider the pressure dependence of the stability limits. Our approximate analysis assumes the independence of the $\{\epsilon_{\alpha\beta}\}$ on pressure and demonstrates that while the spinodals in Figures 2−6 are quite sensitive to pressure, the *relative shifts* $\Delta T_c/T_c(\Phi_3=0)$ and $\Delta\Phi_1^{(c)}/\Phi_1^{(c)}(\Phi_3 = 0)$ in Figures 7−14 change rather slightly with pressure or even remain constant over the range $1.013 \times 10^5 - 1.013 \times 10^8$ Pa.

IV. Conclusions

Many experimental studies of the phase stability of fluid mixtures treat the third component ("impurity") as an unwelcome factor (the "impurity") which could potentially corrupt the measurements on the ideal binary fluid mixtures. It is commonly observed that the additional component significantly alters the phase stability of the fluid mixture, and it is generally assumed that such additives only induce an uninteresting shift in the critical temperature.[7] The systematic study of this "nonuniversal" phenomenon is surprisingly limited, despite the large magnitudes of the observed shifts for the phase boundaries in special cases. Studies of this "dilution effect" are especially important for commercial applications where multicomponent mixtures are the rule rather than the exception. It is essential to know whether under processing conditions a small concentration of some unmonitored impurity component exerts a large influence on the phase stability of the processed material.

A convenient "laboratory" for experimental and theoretical investigation of the dilution effect on phase stability is provided by the addition of diblock copolymers to a homopolymer blend having the same chemical composition. These systems contain many degrees of freedom which can be adjusted (e.g., the lengths of the blocks and homopolymers, the pressure, the monomer shapes) and are therefore more versatile than small molecule fluids for exploring the physical origins of the phase boundary shifts with dilution. By restricting attention to block copolymers with the same chemical composition as the homopolymer blend, the proliferation of energetic parameters is limited to those determined for the pure binary mixtures. This choice then facilitates examination of the influence of block copolymer architecture on the phase stability of the blend. The insights gained from the blend dilution by the block copolymers should extend to more complicated cases of additives having a different chemical composition than that of the blend. We mention, for example, the recent studies by Nesterov et al.[22] for poly(vinyl acetate)/poly-(methyl methacrylate) blends diluted by an inorganic filler. Such mixtures exhibit a demixing due to this additive, an observation which is consistent with the preferential solubility between the diluent and one of the polymer components.[22] The calculations in the present paper indicate that the shape of the irregular diluent particles is as relevant as the specific nature of the chemical interactions between these particles and the blend components. Systematic studies of the geometry and the interactions between the additives and the homopolymers in the blend should provide a better understanding of the dilution effect.

The present lattice cluster theory calculations partially confirm a portion of the phenomenological "Timmermans rule" that additives which are soluble in both mixture components (symmetric diblock copolymers) tend to stabilize a fluid mixture, while impurities which are preferentially soluble in one component tend to destabilize the mixture. We find, however, that when compressibility and monomer structural differences are large, exceptions emerge to this simple rule of thumb for impurity effects on mixing. Specifically, calculations for a PS/PVME blend diluted by a PS-b-PVME diblock predict that both symmetric and asymmetric diblock additives at very low concentrations lead to a large destabilizing influence. Moreover, new types of critical behavior are predicted to appear because of the dilution process. (It is unfortunate that PS-b-PVME diblocks are not currently available to test these predictions of the lattice cluster theory, but similar behavior should also

appear for other LCST type blends.) We note that exceptions of this nature to Timmermans' rule have been observed in small molecule diluted fluid mixtures.[12]

We turn now to considering the applicability of the "universal" relation in eq 1.1, connecting the shifts of the critical temperature and the critical composition in certain diluted small molecule liquids.[9] This relation is found to hold only as a rough approximation for symmetric diblock copolymers having high molecular weights. The approximation appears to become better for symmetric diblock copolymers having low molecular weights, however. No simple correlation exists between the critical composition shift and the critical temperature shift for asymmetric copolymer additives, so we suggest that eq 1.1 has limited universality. It remains a useful approximation for nearly symmetric block copolymers which are important special cases for practical stabilization applications.

We close by mentioning an important aspect of the blend dilution by a diblock copolymer that is difficult to address by the (mean-field) lattice cluster theory. The addition of a diblock copolymer not only is expected to shift the critical temperature and critical composition but can also alter by dilution even the *qualitative type* of phase separation. The addition of symmetric diblock copolymer to a polymer blend should alter the magnitudes of the critical exponents (γ, ν) describing the intensity and scale of the critical fluctuations, as well as the order parameter exponent β determining the qualitative shape of the coexistence curve. This is the Fisher renormalization effect which should be especially large in systems where dilution produces a large shift of the critical temperature for phase separation.[23]

The Fisher renormalization effect is illustrated explicitly in the Wheeler–Widom model[24] of an AA, BB dimer mixture diluted by an AB dimer, a system which is a "cartoon" of the symmetric diblock blend dilution. The net result of the ideal Fisher renormalization upon the critical exponents (γ, ν, β) is that the experimental exponents for the diluted mixture are about $8/7$ times the ideal Ising values.[25] Chu and Lin[26] have carefully studied the dilution effect in small molecule mixtures and have found effective exponents that are even larger than those predicted by Fisher renormalization. Many other studies subsequently have provided similar results. Recent preliminary neutron scattering studies for a PS/PB (polybutadiene) blend qualitatively exhibit[27] the Fisher renormalization effect for a symmetric diblock diluent. Moreover, other types of critical behavior may exist for highly *asymmetric* diblock copolymer diluents. When the block copolymer is very asymmetric or is replaced by a random copolymer, three-phase coexistence and tricritical behavior should then become possible.[28,29] Near a tricritical point the critical behavior is classical with weak logarithmic corrections. The mean-field lattice cluster theory should be especially suitable in describing this type of tricritical three-component mixture. Many recent studies of three-component mixtures consider cases where two components are chemically similar in an effort to study tricritical phenomena.[29] The diblock dilution of a blend provides an ideal system for probing tricritical behavior, but careful experiments require highly monodisperse samples and conditions where micelle formation is absent. By tuning the molecular asymmetry of the diblock copolymer additive, the critical exponents for phase separation might be varied from larger than to smaller than Ising values. Very curious phenomena of this nature seem to have been observed in multicomponent mixtures containing a surfactant component.[30,31] The crossover between differing types of critical behavior should be more amenable to theoretical study in the

case of blend dilution by diblock copolymers because the interaction energies remain the same for all these tuned polymer systems, providing a greatly reduced and more controllable parameter set describing these systems than for surfactant cases studied previously.

Note Added in Proof. Some computations have been done using sets of different $\epsilon_{\alpha\beta}$ which all provide reasonable fits to the PS/PVME scattering data of Han et al. The behavior presented in this paper emerges for $\epsilon_{S-S} < \epsilon_{VME-VME}$, but a somewhat different ternary system phase diagram is found for $\epsilon_{S-S} > \epsilon_{VME-VME}$; namely, the LCST critical temperature shifts vary little upon addition of block copolymer, but the spinodals become quite distorted from the binary blend case as the blend composition moves away from the critical composition. An upper critical solution temperature branch again arises, and the UCST critical temperature is very sensitive to the amount of added block copolymer. Thus, we expect LCST binary blends to display a rich variety of responses to added diblock copolymer.

Appendix: The Noncombinatorial Free Energy of a Ternary A/B/A-*b*-B Polymer Blend

As mentioned in Section II, the noncombinatorial free energy F_{nc} of the ternary A/B/A-*b*-B polymer blend is derived from the lattice cluster theory[13] (LCT) as a polynomial in the actual volume fractions ϕ_i ($i = 1$–3) corresponding to the A, B, and A-*b*-B species, respectively),

$$\frac{F_{nc}}{N_1 k_B T} = \sum_{k=1}^{k^*}\sum_{l=0}^{k}[f_{lk}^{(1,2)}\phi_1{}^l\phi_2{}^{k-l} + f_{lk}^{(1,3)}\phi_1{}^l\phi_3{}^{k-l} +$$
$$f_{lk}^{(2,3)}\phi_2{}^l\phi_3{}^{k-l}] + \sum_{k=1}^{k^*}\sum_{l=1}^{k^*-k-1}\sum_{m=1}^{k^*-k-l}f_{mlk}^{(1,2,3)}\phi_1{}^m\phi_2{}^l\phi_3{}^k \quad (A.1a)$$

The individual terms $f_{lk}^{(i,j)}\phi_i{}^l\phi_j{}^{k-l}$ and $f_{mlk}^{(1,2,3)}\phi_1{}^m\phi_2{}^l\phi_3{}^k$ in eq A.1a describe the correlations between various clusters of bonded and interacting nonbonded monomers chosen from all chains in the system. The coefficients $f_{mlk}^{(1,2,3)} \equiv f_{mlk}$ are obtained from the LCT[13] in the form of double expansions in the inverse lattice coordination number $1/z$ and in the van der Waals attractive nearest neighbor interaction energies $\{\epsilon_{\alpha\beta}/k_B T\}$. The f_{mlk} depend on the monomer structures of the three blend components, the diblock composition m, and on the site occupancy indices M_1, M_2, and M_3. The diagrammatic representation[13] of the LCT produces F_{nc} in the form

$$\frac{F_{nc}}{N_1 k_B T} = \frac{1}{N_1}\ln[1 + \sum_{b,l_{in}}(\text{generalized diagrams})] =$$
$$\frac{1}{N_1}\sum_{b,l_{in}}(\text{generalized cumulant diagrams}) \quad (A.1b)$$

where the generalized cumulant diagrams only contain terms proportional to the first power of N_1 and where the sum over b and l_{in} designates both a sum over all diagrams with b bonds and l_{in} interaction lines and a sum over b and l_{in}. Equations A.1 provide the recipe for generating f_{mlk} by relating these coefficients to particular cumulant diagrams.

We describe here some details of calculating the three-body portion of the noncombinatorial free energy in eq
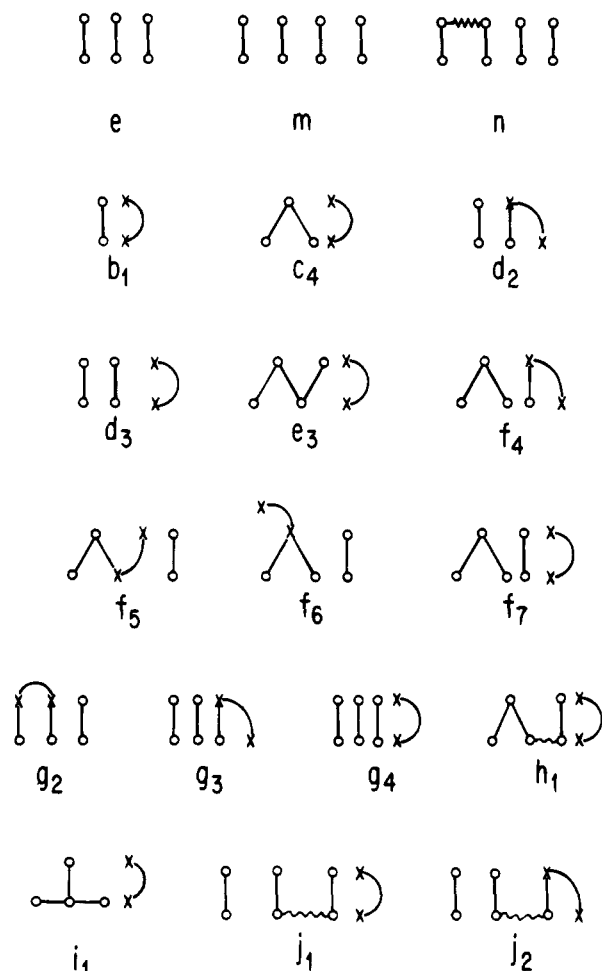
Figure 15. Diagrammatic representation of the three-body portion of the noncombinatorial free energy F_{nc} (see eq A.1a) through orders $1/z^2$ and $\epsilon_{\alpha\beta}/k_BT$. Diagrams contain vertices (circles and crosses) joined by correlating bonds (solid lines) and interaction (curved) lines. The latter designate interactions between a pair of monomer portions which occupy single lattice sites and which are represented by crosses. Wiggly lines in diagrams n, h_1, j_1, and j_2 indicate the bonds lie nonsequentially on a single chain. The cumulant diagrams of eq A.1b are constructed with diagrams e–g_4 as the leading portions.

A.1a through orders $1/z^2$ and $\epsilon_{\alpha\beta}/k_BT$. This simplification fixes the upper limit of k in eq A.1a to $k^* = 5$ and leads to the presence of ten different coefficients f_{mlk} in eq A.1a. The only diagrams contributing to these f_{mlk} must involve at least three correlating bonds (lying on chains of three different polymer species) or an interaction line that is disconnected from at least one correlating bond. In the latter case, the bond and two interacting monomers likewise belong to three different components. Figure 15 displays the leading diagrams of these cumulant diagrams, while the corresponding cumulant diagram contributions $C_{mlk}^{(i)}$ to f_{mlk} are summarized in Table 1. Contributions from cumulant diagrams, whose leading diagrams have a similar topology (such as diagrams n and m, h_1 and f_7, j_2 and g_3, or j_1 and g_4 of Figure 15) must be combined together to eliminate long chain ($M_i \to \infty$) limit divergences in the individual diagrams and to yield a finite free energy in eq A.1a for $M_i \to \infty$. The appearance of this divergence in the individual diagrams stems from the artifical separation for computational convenience of inter- and intramolecular correlations. However, the physical indistinguishability between spatially close bonds, which are distant on the same chain, and those on different chains requires the combining of these pairs of diagrams and leads to a F_{nc} without long chain divergences.

The formulas for $C_{112}^{(i)}$, C_{212}, and C_{113} in Table 1 are expressed in terms of various restricted sums which are identified by primes, double primes, and triple primes. The primes indicate that the summation indices β, γ, and δ in $\sum_{\alpha=A,B,d}\sum_{\beta}'\sum_{\gamma}'\sum_{\delta}'$ are not independent but are related to each other through the conditions

$$\beta \neq \alpha \quad \text{if } \alpha = A, B \qquad (A.2a)$$

$$\begin{cases} \gamma \neq \beta & \text{if } \beta = A, B \text{ or } \beta = \alpha = d \\ \gamma \neq \alpha & \text{if } \alpha = A, B \end{cases} \qquad (A.2b)$$

$$\begin{cases} \delta \neq \gamma & \text{if } \gamma = A, B \text{ or } \gamma = \beta = d \text{ or } \gamma = \alpha = d \\ \delta \neq \beta & \text{if } \beta = A, B \text{ or } \beta = \alpha = d \\ \delta \neq \alpha & \text{if } \alpha = A, B \end{cases} \qquad (A.2c)$$

where A, B, and d denote, respectively, homopolymers A and B and diblock copolymer A-b-B. The double primes on the sums $\sum_{\beta}''\sum_{\gamma}''\sum_{\delta}''\sum_{\eta}''$ in Table 1 designate the restrictions,

$$\beta \neq \alpha \quad \text{if } \alpha = B \qquad (A.3a)$$

$$\begin{cases} \gamma \neq \beta & \text{if } \beta = B \text{ or } \beta = \alpha = A, d \\ \gamma \neq \alpha & \text{if } \alpha = B \end{cases} \qquad (A.3b)$$

$$\begin{cases} \delta \neq \gamma & \text{if } \gamma = B \text{ or } \gamma = \beta = A, d \text{ or } \gamma = \alpha = A, d \\ \delta \neq \beta & \text{if } \beta = B \text{ or } \beta = \alpha = A, d \\ \delta \neq \alpha & \text{if } \alpha = B \end{cases} \qquad (A.3c)$$

$$\begin{cases} \eta \neq \delta & \text{if } \delta = B \text{ or } \delta = \gamma = A, d \text{ or } \delta = \beta = A, d \text{ or} \\ & \qquad \delta = \alpha = A, d \\ \eta \neq \gamma & \text{if } \gamma = B \text{ or } \gamma = \beta = A, d \text{ or } \gamma = \alpha = A, d \\ \eta \neq \beta & \text{if } \beta = B \text{ or } \beta = \alpha = A, d \\ \eta \neq \alpha & \text{if } \alpha = B \end{cases} \qquad (A.3d)$$

while the triple primes on the sums $\sum_{\beta}'''\sum_{\gamma}'''\sum_{\delta}'''\sum_{\eta}'''$ imply the constraints

$$\beta \neq \alpha \quad \text{if } \alpha = A, B \qquad (A.4a)$$

$$\begin{cases} \gamma \neq \beta & \text{if } \beta = A, B \\ \gamma \neq \alpha & \text{if } \alpha = A, B \end{cases} \qquad (A.4b)$$

$$\begin{cases} \delta \neq \gamma & \text{if } \gamma = A, B \text{ or } \gamma = \beta = \alpha = d \\ \delta \neq \beta & \text{if } \beta = A, B \\ \delta \neq \alpha & \text{if } \alpha = A, B \end{cases} \qquad (A.4c)$$

$$\begin{cases} \eta \neq \delta & \text{if } \delta = A, B \text{ or } \delta = \gamma = \beta = d \text{ or } \delta = \gamma = \\ & \qquad \alpha = d \text{ or } \delta = \beta = \alpha = d \\ \eta \neq \gamma & \text{if } \gamma = A, B \text{ or } \gamma = \beta = \alpha = d \\ \eta \neq \beta & \text{if } \beta = A, B \\ \eta \neq \alpha & \text{if } \alpha = A, B \end{cases} \qquad (A.4d)$$

A comparison of Table 1 with the previous results[13,32] for multicomponent homopolymer blends indicates the presence of a formal resemblence between the cumulant diagram contributions for A/B/A-b-A and A/B/C ternary systems. The isomorphism between these two cases is defined by the relations[33]

$$M_d \leftrightarrow M_C$$

$$N_i^{(d_A)} + N_i^{(d_B)} + a_i \leftrightarrow N_i^{(C)}$$

Table 1. Calculation of the Helmholtz Free Energy Coefficients $f_{lkm}^{1,2,3}$ through Orders $1/z^2$ and $\epsilon_{\alpha\beta}/k_BT$ for the Ternary Polymer Blend A/B/A-b-B

diagrams shown in Figure 15	$C_{lkm}^{(i)}$ contribution from corresponding cumulant diagram[13] to $f_{lkm}^{1,2,3}$	
e	$C_{111}^{(1)} = -\dfrac{8}{3z^2}\sum_{\alpha=A,B,d}\sum_{\beta\neq\alpha}\sum_{\gamma\neq\alpha,\beta}N(1,\alpha)N(1,\beta)N(1,\gamma)$	
n + m	$C_{111}^{(2)} = -\dfrac{4}{z^2}\sum_{\alpha=A,B,d}\sum_{\beta\neq\alpha}\sum_{\gamma\neq\alpha,\beta}N(1,\alpha)N(1,\beta)N'(1,2;\gamma)$	
$b_1 + c_4 + e_3 + i_1$	$C_{111}^{(3)} = \sum_{\alpha=A,B,d}\left[-N(1,\alpha)+\dfrac{2}{z}N(2,\alpha)+\dfrac{1}{z}N(3,\alpha)+\dfrac{3}{z}N(\perp,\alpha)\right]\sum_{\beta\neq\alpha}\sum_{\gamma\neq\alpha,\beta}\epsilon_{\beta\gamma}^{(1)}$	
d_2	$C_{111}^{(4)} = \dfrac{8}{z}\sum_{\alpha=A,B,d}\sum_{\beta\neq\alpha}N(1,\alpha)N(1,\beta)\sum_{\gamma\neq\alpha,\beta}\epsilon_{\alpha\gamma}^{(2)}$	
$f_4 + f_5 + f_6 + f_7 + h_1$	$C_{111}^{(5)} = -\dfrac{4}{z}\sum_{\alpha=A,B,d}\sum_{\beta\neq\alpha}N(1,\alpha)N(2,\beta)\sum_{\gamma\neq\alpha,\beta}\left[\epsilon_{\alpha\gamma}^{(2)}-\epsilon_{\beta\gamma}^{(3)}-\dfrac{3}{2}(\epsilon_{\beta\gamma}^{(4)}-\epsilon_{\beta\gamma}^{(5)})\right]+\dfrac{1}{z}\sum_{\alpha=A,B,d}N'(1,2;\alpha)\sum_{\beta\neq\alpha}\sum_{\gamma\neq\alpha,\beta}\epsilon_{\beta\gamma}^{(1)}$	
$g_2 + g_3 + j_2$	$C_{111}^{(6)} = \dfrac{8}{z}\sum_{\alpha=A,B,d}\sum_{\beta\neq\alpha}N(1,\alpha)N'(1,1;\beta)\sum_{\gamma\neq\alpha,\beta}\epsilon_{\beta\gamma}^{(6)}-\dfrac{4}{z}\sum_{\alpha=A,B,d}\sum_{\beta\neq\alpha}\sum_{\gamma\neq\alpha,\beta}N(1,\alpha)N(1,\beta)N(1,\gamma)[\epsilon_{\alpha\beta}^{(2)}\delta^{Kr}(\gamma-d)+$ $\epsilon_{\beta\alpha}^{(2)}\delta^{Kr}(\beta-d)+\epsilon_{\beta\alpha}^{(2)}\delta^{Kr}(\alpha-d)]$	
m	$C_{112}^{(1)} = -\dfrac{2}{z^2}\sum_{\alpha=A,B,d}\sum_{\beta}{}'\sum_{\gamma}{}'\sum_{\delta}{}'N(1,\alpha)N(1,\beta)N(1,\gamma)N(1,\delta)$	(1)
d_3	$C_{112}^{(2)} = -\dfrac{4}{z}\sum_{\alpha=A,B,d}\sum_{\beta}{}'N(1,\alpha)N(1,\beta)\sum_{\gamma}{}'\sum_{\delta}{}'\epsilon_{\gamma\delta}^{(1)}$	(2)
$g_4 + j_1$	$C_{112}^{(3)} = \dfrac{8}{z}\sum_{\alpha=A,B,d}\sum_{\beta}{}'\sum_{\gamma}{}'N(1,\alpha)N(1,\beta)N(1,\gamma)\sum_{\delta}{}'\epsilon_{\alpha\delta}^{(2)}-\dfrac{4}{z}\sum_{\alpha=A,B,d}\sum_{\beta}{}'N(1,\alpha)N'(1,1;\beta)\sum_{\gamma}{}'\sum_{\delta}{}'\epsilon_{\gamma\delta}^{(1)}$	(3)
g_4	$C_{122} = -\dfrac{4}{z}\sum_{\alpha=A,B,D}\sum_{\beta}{}''\sum_{\gamma}{}''N(1,\alpha)N(1,\beta)N(1,\gamma)\sum_{\delta}{}''\sum_{\eta}{}''\epsilon_{\delta\eta}^{(1)}$	(4)
	$C_{113} = -\dfrac{4}{z}\sum_{\alpha=A,B,d}\sum_{\beta}{}'''\sum_{\gamma}{}'''N(1,\alpha)N(1,\beta)N(1,\gamma)\sum_{\delta}{}'''\sum_{\eta}{}'''\epsilon_{\delta\eta}^{(1)}$	(5)

where

$N(i,\alpha) = N_i^{(\alpha)}/M_\alpha \qquad \alpha = A, B \quad i = 1, 2, 3, \perp$

$N(i,d) = (N_i^{(d_A)} + N_i^{(d_B)} + a_i)/M_d \qquad M_d = M_d^{(A)} + M_d^{(B)} \quad i = 1, 2, 3, \perp$

$N'(i,j;\alpha) = [N_{ij}^{(\alpha)} - (1/2)^{\delta^{Kr}(i-j)}N_i^{(\alpha)}N_j^{(\alpha)}]/M_\alpha \qquad \alpha = A, B \quad i,j = 1, 2$

$N'(i,j;d) = [N_{ij}^{(d_A)} + N_{ij}^{(d_B)} - \alpha_{ij} - (1/2)^{\delta^{Kr}(i-j)}[N_i^{(d_A)}N_j^{(d_A)} + N_i^{(d_B)}N_j^{(d_B)} + \alpha_i\alpha_j]]/M_d \qquad i,j = 1, 2$

$\epsilon_{AB}^{(i)} = \epsilon_{AB} \qquad i = 1, 2, ..., 6$

$\epsilon_{\alpha d}^{(i)} = \epsilon_{\alpha d} = \epsilon_{A\alpha}m + \epsilon_{\alpha B}(1 - m) \qquad m = M_d^{(A)}/M_d \qquad \alpha = A, B \quad i = 1, 2, ..., 6$

$\epsilon_{dd}^{(1)} = \epsilon_{AA}m^2 + \epsilon_{BB}(1 - m)^2 + 2\epsilon_{AB}m(1 - m)$

$\epsilon_{dd}^{(2)} = \epsilon_{dA}^{(2)}m + \epsilon_{dB}^{(2)}(1 - m)$

$\epsilon_{d\alpha}^{(i)} = \epsilon_{A\alpha}x^{(i)} + \epsilon_{\alpha B}(1 - x^{(i)}) \qquad \alpha = A, B \quad i = 2, 3, ..., 6$

$\epsilon_{d\alpha}^{(1)} = \epsilon_{\alpha d}$

$x^{(2)} = \dfrac{N_1^{(d_A)} + 1/2}{N_1^{(d_A)} + N_1^{(d_B)} + 1} \qquad x^{(3)} = \dfrac{N_2^{(d_A)} + (1/2)a_2}{N_2^{(d_A)} + N_2^{(d_B)} + a_2} \qquad x^{(4)} = \dfrac{N_2^{(d_A)} + r_2 a_2}{N_2^{(d_A)} + N_2^{(d_B)} + a_2} \qquad x^{(5)} = \dfrac{N_2^{(d_A)} + (1/3)[1 + r_2]a_2}{N_2^{(d_A)} + N_2^{(d_B)} + a_2}$

$x^{(6)} = \dfrac{N_{11}^{(d_A)} - (1/2)[N_1^{(d_A)}]^2 - (1/4)[1 + 2r_{11}]a_{11} - 1/4}{N_{11}^{(d_A)} - (1/2)[N_1^{(d_A)}]^2 + N_{11}^{(d_B)} - (1/2)[N_1^{(d_B)}]^2 - a_{11} - 1/2}$

The indices A, B, d, d_A, and d_B designate, respectively, homopolymers A and B, diblock copolymer A-b-B, and its blocks A and B. Consequently, M_A, M_B, $M_d^{(A)}$, $M_d^{(B)}$, and M_d denote the site occupancy indices for these species; $N_i^{(A)}$, $N_i^{(B)}$, $N_i^{(d_A)}$, and $N_i^{(d_B)}$ ($i = 1$–3) are the numbers of sets of i sequential bonds in a single chain or in a block; $N_\perp^{(A)}$, $N_\perp^{(B)}$, $N_\perp^{(d_A)}$, and $N_\perp^{(d_B)}$, are the numbers of distinct sets of three bonds which meet simultaneously at a single lattice site; and $N_{ij}^{(A)}$, $N_{ij}^{(B)}$, $N_{ij}^{(d_A)}$, and $N_{ij}^{(d_B)}$ represent numbers of ways for selecting two nonsequential sets of i and j sequential bonds from $N_1^{(\alpha)}$ ($\alpha = A, B, d_A$, and d_B) bonds. The geometrical coefficients[33] a_i ($i = 1$–3) and $a_\perp$ enumerate similar sets of bonds that contain the junction bond, whereas the definition of a_{ij} includes all overlapping configurations of two sets of i and j sequential bonds, such that one set contains the junction bond, whereas the other pertains to either block. The fractions r_2 and r_{11} specify[33] respectively the portions of a_2 and a_{11} that belong to the block A, and all energies $\epsilon_{\alpha\beta}$ are expressed in units of k_BT.

$$N_{ij}^{(d_A)} + N_{ij}^{(d_B)} + (1/2)^{\delta^{Kr}(i-j)}[N_i^{(d_A)}N_j^{(d_B)} + N_i^{(d_B)}N_j^{(d_A)} +$$
$$(N_i^{(d_A)} + N_i^{(d_B)})a_j + (N_j^{(d_A)} + N_j^{(d_B)})a_i] \leftrightarrow N_{ij}^{(C)}$$

$$\epsilon_{Ad} \equiv \epsilon_{AA}m + \epsilon_{AB}(1-m) \leftrightarrow \epsilon_{AC}$$

$$\epsilon_{Bd} \equiv \epsilon_{AB}m + \epsilon_{BB}(1-m) \leftrightarrow \epsilon_{BC}$$

and

$$\epsilon_{dd}^{(i)} \leftrightarrow \epsilon_{CC} \qquad i = 1, 2$$

where δ^{Kr} is the Kronecker delta and where the combinatorial factors and interaction energy parameters on the left-hand sides apply to diblock copolymers $d \equiv A\text{-}b\text{-}B$, as explained in detail in Table 1, while those with superscript (C) or subscrips C, AC, BC, or CC on the right-hand sides are the corresponding quantities for homopolymer species C in the ternary A/B/C blend.

The four main coefficients f_{111}, f_{112}, f_{113}, and f_{212} are obtained by summing the appropriate $C_{mlk}^{(i)}$ of Table 1 as

$$f_{111} = \sum_{i=1}^{6} C_{111}^{(i)} \qquad (A.5a)$$

$$f_{112} = \sum_{i=1}^{3} C_{112}^{(i)} \qquad (A.5b)$$

$$f_{212} = C_{212} \qquad (A.5c)$$

and

$$f_{113} = C_{113} \qquad (A.5d)$$

while the six other f_{mlk} follow from eqs A.6 and the expressions of Table 1 by using simple symmetry arguments. For instance, f_{121} is symmetrically related to f_{112} and is given by the same eq A.6b with the only modification for $C_{112}^{(i)}$ involving the interchange of indices d and B in the conditions (A.2). This process can be schematically written as

$$f_{112} \rightarrow f_{121} \text{ by } d \rightleftharpoons B \text{ in (A.2)}$$

and

$$f_{112} \rightarrow f_{211} \text{ by } d \rightleftharpoons A \text{ in (A.2)}$$

A similar procedure may be applied to the constraints (A.3) and (A.4) to yield f_{122}, f_{221}, f_{131}, and f_{311} from eqs 4 and 5 in Table 1. The process is illustrated in symbolic notation as

$$f_{212} \rightarrow f_{122} \text{ by } A \rightleftharpoons B \text{ in (A.3)}$$

$$f_{212} \rightarrow f_{221} \text{ by } d \rightleftharpoons B \text{ in (A.3)}$$

$$f_{113} \rightarrow f_{311} \text{ by } d \rightleftharpoons A \text{ in (A.4)}$$

and

$$f_{113} \rightarrow f_{131} \text{ by } d \rightleftharpoons B \text{ in (A.4)}$$

References and Notes

(1) Scott, R. L. *J. Chem. Phys.* **1949**, *17*, 279.
(2) Roe, R. J.; Rigby, D. *Adv. Polym. Sci.* **1987**, *82*, 105 (see the Introduction of this paper for a historical commentary).
(3) Kawakatsu, T.; Kawasaki, K.; Furusaka, M.; Okabayashi, H.; Kanaya, T. *J. Chem. Phys.* **1993**, *99*, 8200. (See ref 12 of this paper for experimental evidence of the dilution effect on blend phase separation kinetics.) Grest, G. S.; Srolowitz, D. J. *Phys. Rev. B* **1985**, *32*, 3014.

(4) Noolandi, J.; Hong, K. M. *Macromolecules* **1982**, *15*, 482. Noolandi, J. *Macromol. Chem., Rapid Commun.* **1991**, *12*, 517.
(5) Wang, Z.-W.; Safran, S. A. *J. Phys. (Paris)* **1990**, *51*, 185.
(6) Anisimov, M. A.; Gorodetsky, E. E.; Davdov, A. J.; Kurliandsky A. S. *Int. J. Thermophys.* **1992**, *13*, 921.
(7) Tveekrem, J. L.; Jacobs, D. T. *Phys. Rev. A* **1983**, *27*, 2773.
(8) Cohn, R. H.; Jacobs, D. T. *J. Chem. Phys.* **1984**, *80*, 856.
(9) Jacobs, D. T. *J. Chem. Phys.* **1989**, *91*, 560.
(10) Takebe, T.; Sawaoka, R.; Hashimoto, T. *J. Chem. Phys.* **1989**, *91*, 4369. Tveekrem, J. T.; Greer, S. C.; Jacobs, D. T. *Macromolecules* **1988**, *21*, 147.
(11) Timmermans, J. *Z. Phys. Chem.* **1907**, *58*, 129. See also: Prigogine, I.; Defay, R. *Chemical Thermodynamics*: Longmans: Birmingham, AL, 1967; p 256.
(12) Hales, B. J.; Bertrand, G. L.; Hepler, L. G. *J. Phys. Chem.* **1966**, *70*, 3970.
(13) Dudowicz, J.; Freed, K. F. *Macromolecules* **1991**, *24*, 5074.
(14) Dudowicz, J.; Freed, M. S.; Freed, K. F. *Macromolecules* **1991**, *24*, 5096. Nemirovsky, A. M.; Bawendi, M. G.; Freed, K. F. *J. Chem. Phys.* **1987**, *87*, 7272.
(15) Freed, K. F.; Dudowicz, J. Unpublished work.
(16) Tompa, H. *Polymer Solution*; Butterworths Scientific Publications: London, 1956. Bergmann, J.; Kehlen, H.; Ratzsch, M. *J. Phys. Chem.* **1987**, *91*, 6567. Lifschitz, M.; Dudowicz, J.; Freed, K. F. *J. Chem. Phys.* **1994**, *100*, 3957.
(17) Sanchez, I. C. *Macromolecules* **1991**, *24*, 908.
(18) Dudowicz, J.; Lifschitz, M.; Freed, K. F.; Douglas, J. F. *J. Chem. Phys.* **1993**, *99*, 4804.
(19) Dudowicz, J.; Freed, K. F. *Macromolecules* **1991**, *24*, 5112.
(20) Dudowicz, J.; Freed, K. F.; Lifschitz, M. *Macromolecules* **1994**, *27*, 5387.
(21) Freed, K. F.; Dudowicz, J. *J. Chem. Phys.* **1992**, *97*, 2105.
(22) Nesterov, A. E.; Lipatov, Y.; Horichko, V. V.; Gritsenko, O. T. *Polymer* **1992**, *33*, 619.
(23) Fisher, M. E. *Phys. Rev.* **1968**, *176*, 257. Fisher, M. E.; Scesney, P. E. *Phys. Rev. A* **1970**, *2*, 825. Lipa, B. J.; Buckingham, M. J. *Phys. Lett. A* **1968**, *26*, 643. Essam, J. W.; Garelick, H. *Proc. Phys. Soc.* **1967**, *92*, 136. Syozi, I.; Miyazima, S. S. *Prog. Theor. Phys. Jpn.* **1966**, *36*, 1083.
(24) Wheeler, J. C.; Widom, B. *J. Am. Chem. Soc.* **1968**, *90*, 3064.
(25) Sengers, J. V.; Levelt Sengers, J. M. H. *Annu. Rev. Phys. Chem.* **1986**, *37*, 189.
(26) Chu, B.; Lin, F. L. *J. Chem. Phys.* **1975**, *61*, 5132. Ohbayashi, K.; Chu, B. *J. Chem. Phys.* **1978**, *68*, 5066.
(27) Nakatani, A. I. *Am. Phys. Soc. (March Meet.)* **1994**. Yajima, H.; Hair, D. W.; Nakatani, A. I.; Douglas, J. F.; Han, C. C. *Phys. Rev. B* **1993**, *47*, 12268.
(28) Sundar, G.; Widom, B. *Fluid Phase Equilib.* **1988**, *40*, 289. Pegg, I. L.; Knobler, C. M.; Scott, R. L. *J. Chem. Phys.* **1990**, *92*, 5442. Sadus, R. *J. Phys. Chem.* **1992**, *96*, 5197.
(29) Broseta, D.; Fredrickson, G. H. *J. Chem. Phys.* **1990**, *93*, 2927.
(30) Belocq, A. M.; Honorat, P.; Roux, D. *J. Phys. (Paris)* **1985**, *46*, 743.
(31) Aschauer, R.; Beysens, D. *Phys. Rev. E* **1993**, *47*, 1850.
(32) The correct forms of the following cumulant diagram contributions from Tables 1 and 2 of ref 13 are

$$C_{22}^{(\epsilon)} = -\frac{3}{2}C_{20}^{(\epsilon)} + \frac{1}{z}\sum_{\kappa=1}^{k} N(1,\kappa)N(2,\kappa)M_\kappa\phi_\kappa \sum_{\mu=1}^{k}\sum_{\eta=1}^{k}\epsilon_{\mu\eta}\phi_\mu\phi_\eta$$

$$C_{32}^{(\epsilon^2)} = -C_{24}^{(\epsilon^2)} + 2\sum_{\kappa=1}^{k}[N(1,\kappa)]^2 M_\kappa\epsilon_{\kappa\kappa}\phi_\kappa\sum_{\mu=1}^{k}\epsilon_{\kappa\mu}\phi_\mu$$

The second terms of $C_{19}^{(\epsilon)}$ and $C_{38}^{(\epsilon^2)}$ should respectively read

$$-\frac{6}{z}\sum_{\kappa=1}^{k}\sum_{\lambda=1}^{k}N(1,\kappa)N(2,\lambda)\phi_\kappa\phi_\lambda\epsilon_{\kappa\lambda}$$

$$-2\sum_{\kappa=1}^{k}\sum_{\lambda=1}^{k}N(1,\kappa)N(1,\lambda)\phi_\kappa\phi_\lambda\sum_{\mu=1}^{k}\sum_{\eta=1}^{k}\sum_{\omega=1}^{k}[\epsilon_{\mu\eta}\epsilon_{\eta\omega} + 4\epsilon_{\kappa\mu}\epsilon_{\eta\omega}]\phi_\mu\phi_\eta\phi_\omega$$

(33) Dudowicz, J.; Freed, K. F. *J. Chem. Phys.* **1994**, *100*, 4653.